Dalton Transactions

RSC Publishing

PAPER

View Article Online
View Journal | View Issue

Cite this: *Dalton Trans.*, 2013, **42**, 16762

Polymerization of propylene promoted by zirconium benzamidinates†

Sinai Aharonovich, Naveen V. Kulkarni, Jia-Sheng Zhang, Mark Botoshansky, Moshe Kapon and Moris S. Eisen*

Received 25th June 2013,
Accepted 2nd September 2013

DOI: 10.1039/c3dt51688a

www.rsc.org/dalton

New bis(*N*,*N*-trimethylsilylarylamidinate) zirconium dichloride complexes with various carbon substituents were prepared, and their solid as well as solution state structures were studied. In the polymerization of propylene, after activation by MAO, these catalysts provided two fractions. Ether soluble polymers were obtained at a low activity as sticky polymers with lower molecular weights, except with the *o*-OMe substituted complex. The solid fractions were composed of a highly isotactic polymer and a moderately syndiotactic polymer. An interesting linear correlation was found between the rates of the 2,1 and 3,1 insertions for the ether soluble fractions.

Introduction

During the past few decades, the research area of olefin polymerization has advanced significantly, with the development of homogeneous group 4 metallocene catalysts,[1–3] half-metallocene[4–6] and many other complexes containing interesting chelating ancillary ligands.[7–9] Among these chelating ligands, amidinates are of particular interest due to the simplicity with which they can be modified, producing ligands with specific steric and electronic properties.[10] In addition, the rich coordination chemistry has made this class of ancillary ligands attractive for the production of various organometallic complexes useful for the polymerization of α-olefins.[11]

We have demonstrated that group 4 bis(benzamidinate) dichloride and dialkyl complexes, when activated by methylaluminoxane (MAO), form catalytically active species which can polymerize propylene, affording a mixture of isotactic and elastomeric polypropylenes.[12,13] The mechanistic studies have suggested that the activation of the benzamidinate complex (**I** in Scheme 1) takes place in two parallel pathways. The first route involves the formation of a cationic bis-amidinate alkyl complex as an active species, responsible for the formation of the isotactic fraction (**II** in Scheme 1). The second route involves the formation of a cationic mono-amidinate dialkyl complex, resulting from ligand dissociation of the bis-amidinate complex and its migration to aluminium in MAO, producing the elastomeric fraction (**V** *via* **III** and **IV** in Scheme 1).[12]

The mechanistic studies revealed that the mono(amidinate) complex (**III**) responds to the ligand migration by rearranging the remaining amidinate, resulting in the reattachment of this moiety to the metal *via* one nitrogen atom and a π-bonded phenyl ring (**V**). Further it is seen that when comparing the simple titanium bis(phenylamidinate) complex to the titanium bis(*p*-tolylamidinate) complex, a polypropylene with a much higher molecular weight and a complex with a reduced catalytic activity were obtained in the latter case. It is envisaged that, after the rearrangement of the ligand, the *para*-substituent interacts with a growing polymer chain, impeding the chain termination and allowing higher molecular weights (**VI** in Scheme 1). Varying the substituents at the *para* position of the aryl group revealed that bulkier substituents lead to the formation of polymers with higher molecular weights, exhibiting a linear free energy relationship between the *para*-substituent and the Taft parameters.[14,15]

The detailed studies of the various group 4 olefin polymerization catalysts developed recently have revealed that the activity of the catalyst and the properties of the polymer produced are highly dependent on the nature of the central metal atom.[16,17] In particular, when the Ti and Zr complexes with the same ligands are compared, a surprising difference in their reactivity for the polymerization of α-olefins and in the properties of the obtained polymers was found.[18]

Herein, we present our studies on the solid state and the solution structure of various substituted zirconium bis(benzamidinates). We will present several important key factors in the catalytic polymerization process promoted by these complexes, which have a significant influence on the properties of the obtained polymers such as propylene insertion rates (related

Schulich Faculty of Chemistry, Institute of Catalysis Science and Technology, Technion – Israel Institute of Technology, Technion City, 32000 Haifa, Israel. E-mail: chmoris@tx.technion.ac.il

†Electronic supplementary information (ESI) available. CCDC 946660–946664. For ESI and crystallographic data in CIF or other electronic format see DOI: 10.1039/c3dt51688a

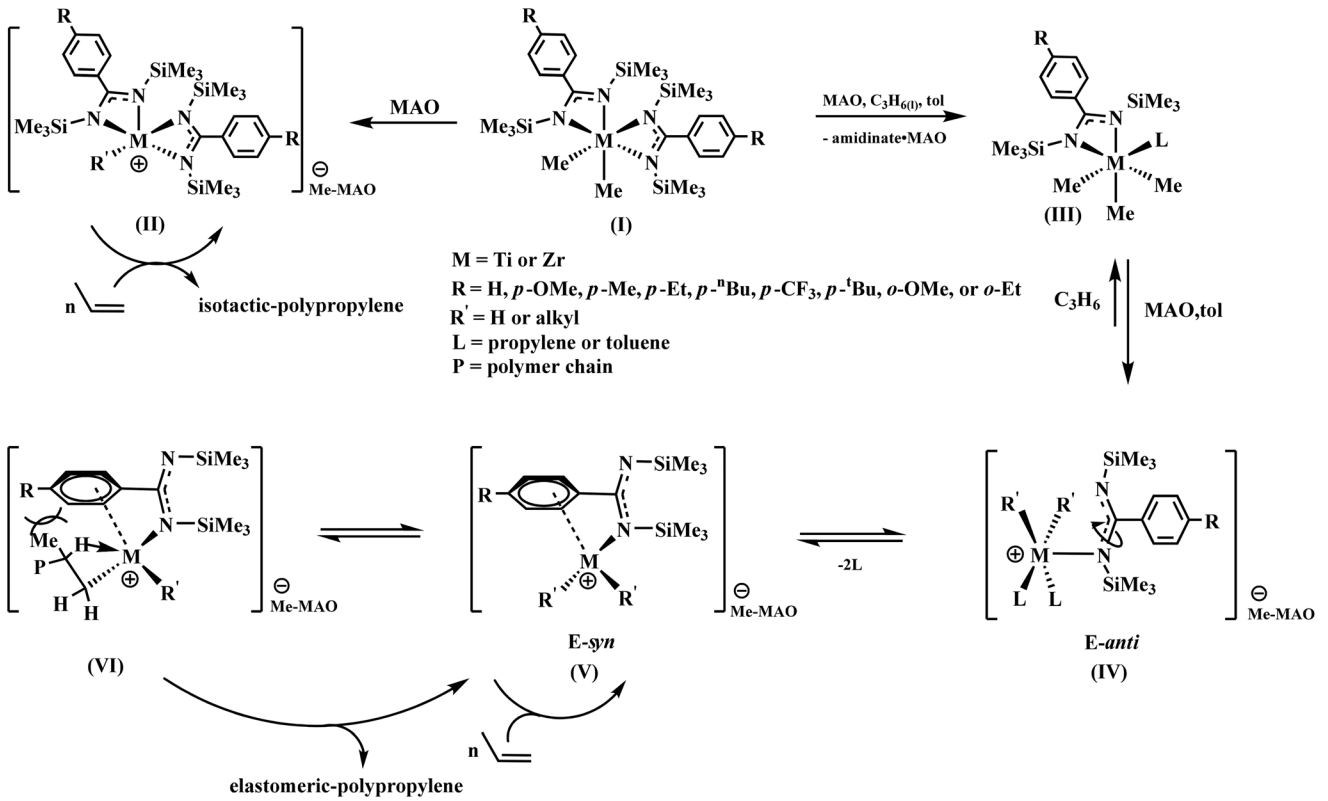

Scheme 1 Plausible mechanism for the formation of the mixture of isotactic and elastomeric polypropylenes by the (benzamidinate) complexes.

to the catalytic activity), chain termination rates (which together with the rate of insertion determine the polymer molecular weight), the stereoregularity of the polymer, the regioregularity (2,1 *vs.* 3,1 insertion rates) and polydispersity.

The *ipso*-C-substitution effect for aryl substituents was evaluated using phenyl based systems with substituents of diverse steric and electronic properties, at different positions on the aromatic ring and replacement of the phenyl ring with a furyl ring. The effect of the replacement of the metal centre by zirconium on the activities and properties of the obtained polymers, as compared to the previously reported titanium complexes, is presented.[14]

Experimental

General procedures

All manipulations of air-sensitive materials were performed with the careful exclusion of oxygen and moisture in flamed Schlenk type glassware on a dual-manifold Schlenk line, or interfaced to a high-vacuum (10^{-5} Torr) line, or in a nitrogen-filled "M-Braun" or "Vacuum Atmospheres" glove box with a medium-capacity recirculator (1–2 ppm O_2).

Argon and nitrogen gases were purified by passing them through a MnO oxygen-removal column and a Davison 4 Å activated molecular sieve column. All the common and deuterated solvents (THF, toluene, hexane, and toluene-d_8) were distilled and stored over Na/K alloy.

The NMR spectra were recorded using Bruker AM 300 and AM 500 spectrometers. Chemical shifts for ^{1}H and ^{13}C were referenced to internal solvent resonances and are reported relative to TMS. NMR experiments for the air sensitive metal complexes were conducted on Teflon valve-sealed tubes (J-Young) after vacuum transfer of the solvent in a high-vacuum line. The NMR experiments for polypropylenes were carried out in tetrachloroethylene-d_2 (TCE) at 363 K on 300 or 500 MHz NMR spectrometers.

X-ray data were acquired on a single-crystal material, which was immersed in Paratone-N oil and quickly fished with a glass rod and mounted on a Kappa CCD diffractometer under a cold stream of nitrogen. Data collection was performed using monochromated MoKα radiation using φ and ω scans to cover the Ewald sphere.[19] Accurate cell parameters and refinement data were obtained with the amount of indicated reflections (Tables 1 and 2).[20] The structure was solved by SHELXS-97 direct methods,[21] and refined using the SHELXL-97 program package.[22] The atoms were refined anisotropically and hydrogen atoms were included using the riding model. Software used for molecular graphics: ORTEP 3.1.[23]

Melting points of the polymers were measured by DSC (Polymer Laboratories, UK) from the second heating thermogram (heating rate – 10 °C min^{-1}). Molecular weights and polydispersities of polymers were determined by the GPC method on the Waters-Alliance 2000 instrument using 1,2,4-trichlorobenzene as a mobile phase at 160 °C. Polystyrene standards

Table 1 Crystal data and refinement details for complexes **9–11**

Complex	**9**	**10**	**11**
Empirical formula	$C_{28}H_{50}Cl_2N_4O_2Si_4Zr$	$C_{30}H_{54}Cl_2N_4Si_4Zr$	$C_{102}H_{186}Cl_6N_{12}Si_{12}Zr_3$
Formula weight	749.20	745.25	2404.08
Temperature (K)	230.0(1) K	230.0(1)	230.0(1)
Wavelength (Å)	0.71073	0.71073	0.71073
Crystal system,	Triclinic	Monoclinic	Monoclinic
Space group	$P\bar{1}$	$C2/c$	$P21/n$
Unit cell dimensions	a = 11.1770(3) Å b = 13.2410(4) Å c = 15.1640(5) Å α = 64.6330(15)° β = 88.4740(15)° γ = 72.6430(15)°	a = 28.3540(11) Å b = 8.8490(5) Å c = 20.4080(10) Å α = 90° β = 128.046(3)° γ = 90°	a = 18.8580(2) Å b = 22.1300(3) Å c = 32.6300(4) Å α = 90° β = 98.5150(11)° γ = 90°
Volume (Å^3)	1922.11(10)	4032.4(3)	13 467.3(3)
z, calculated density (Mg m^{-3})	2, 1.294	4, 1.228	4, 1.186
Absorption coefficient (mm^{-1})	0.579	0.548	0.497
F(000)	784	1568	5088
Crystal size (mm)	0.36 × 0.30 × 0.09	0.24 × 0.16 × 0.12	0.27 × 0.20 × 0.12
θ range for data collection	1.50–27.47	1.82–25.05	1.12–23.00
Limiting indices	$-14 \le h \le 14$, $-17 \le k \le 17$, $-19 \le l \le 19$	$-33 \le h \le 33$, $-10 \le k \le 10$, $-24 \le l \le 24$	$0 \le h \le 20$, $0 \le k \le 24$, $-35 \le l \le 35$
Reflections collected/unique	14 549/8760 [R(int) = 0.0357]	6258/3544 [R(int) = 0.0467]	18 690/18 690 [R(int) = 0.0000]
Completeness to highest θ	99.3%	98.9%	99.7%
Refinement method	Full-matrix least-squares on F^2	Full-matrix least-squares on F^2	Full-matrix least-squares on F^2
Data/restraints/parameters	8760/0/380	3544/0/187	18 690/0/1226
Goodness-of-fit on F^2	0.969	0.941	1.009
Final R indices [$I > 2\sigma(I)$]	R_1 = 0.0415, wR_2 = 0.1094	R_1 = 0.0402, wR_2 = 0.0957	R_1 = 0.0551, wR_2 = 0.1257
R indices (all data)	R_1 = 0.0669, wR_2 = 0.1164	R_1 = 0.0648, wR_2 = 0.1010	R_1 = 0.1334, wR_2 = 0.1463
Largest diff. peak and hole (e Å^{-3})	0.538 and −0.709	0.330 and −0.471	0.444 and −0.338

were used for the standard calibration curve of the GPC. Elemental analyses of all the compounds were carried out using a Flash 2000 CHNS analyser or at the microanalysis laboratory of the Hebrew University of Jerusalem.

$ZrCl_4$ (Sigma) and all other reagents were purchased from Aldrich and Fluka. All the chemicals were used without further purification unless otherwise stated. [4-OMeC$_6$H$_4$C(NSiMe$_3$)$_2$]-Li·TMEDA (**2**), [4-EtC$_6$H$_4$C(NSiMe$_3$)$_2$]Li·TMEDA (**3**) and [4-^{n}BuC$_6$H$_4$C(NSiMe$_3$)$_2$]Li·TMEDA (**4**), [2-OMeC$_6$H$_4$C(NSiMe$_3$)$_2$]-Li·TMEDA (**5**), [3-OMeC$_6$H$_4$C(NSiMe$_3$)$_2$]Li·TMEDA (**6**),[24] [(3-C$_4$H$_3$O)C(NSiMe$_3$)$_2$] Li·TMEDA (**7**)[25] and [C$_6$H$_5$C(NSiMe$_3$)$_2$]$_2$-ZrCl$_2$ (**8**)[26,27] were prepared by the methods reported in the literature.

General procedure for syntheses of bis(arylamidinate) zirconium dichloride complexes (9–14)

To a swivel frit equipped with two 100 mL flasks, 0.466 g (2 mmol) of $ZrCl_4$ was added inside the glove box. The frit was connected to a high vacuum line, and the solids were suspended in 35 mL of toluene, which was cooled to 0 °C. 4 mmol of the lithium compound (**1–7**) was dissolved in 20 mL of toluene, and the solution was injected dropwise to the frit. The colorless-to-faint-yellow suspension which resulted was stirred for 3 h, after which the reaction mixture was evaporated, and TMEDA was removed by low-pressure azeotrope distillations with toluene. The resulting solids were extracted with toluene (3 × 20 mL), and the extract was filtered. The volume of the filtrate was reduced until turbidity was noted, and the concentrated solution was warmed to room temperature to obtain a clear solution and cooled gradually to −30 °C for up to 72 h, to yield crystals of the product. The crystals were separated from the mother liquor by decantation, washed twice with a small amount of cold hexane and dried with a gentle stream of argon.

[4-OMeC$_6$H$_4$C(NSiMe$_3$)$_2$]$_2$ZrCl$_2$ (9)

1.667 g (4 mmol) of compound **2** gave 1.169 g (78% yield) of **9**.

^{1}H NMR (300 MHz, toluene-d_8): δ = 7.12 (d, ^3J = 8.7 Hz, 4H, Ph), 6.60 (d, ^3J = 8.7 Hz, 4H, ph), 3.24 (s, 6H, CH_3-O), 0.23 (s, 36H, CH_3Si).

^{13}C NMR (75.5 MHz, toluene-d_8): δ = 186.8 (N-*C*-N), 162.3, 133.8, 129.2, 115.1 (Ph), 56.1 (*C*H$_3$-O), 3.5 (*C*H$_3$Si).

Elemental analysis data for $C_{28}H_{50}N_4Cl_2O_2Si_4Zr$ (749.20): calculated: C, 44.89; H, 6.73; N, 7.48; Cl; 9.46. Found: C, 42.76; H, 6.94; N, 7.42; Cl, 10.67.

[4-EtC$_6$H$_4$C(NSiMe$_3$)$_2$]$_2$ZrCl$_2$ (10)

1.659 g (4 mmol) of compound **3** gave 1.237 g (83% yield) of **10**.

^{1}H NMR (300 MHz, toluene-d_8): δ = 7.16 (d, ^3J = 7.9 Hz, 4H, Ph), 6.89 (d, ^3J = 7.9 Hz, 4H, Ph) 2.37 (q, ^3J = 7.6 Hz, 4H, CH_2-Ph), 1.04 (t, ^3J = 7.6 Hz, 6H, CH_3), 0.22 (s, 36H, CH_3Si).

^{13}C NMR (75.5 MHz, toluene-d_8): δ = 185.3 (N-*C*-N), 146.0, 137.3, 127.8, 126.3 (Ph), 28.9(*C*H$_2$-Ph), 15.5 (*C*H$_3$), 2.0 (*C*H$_3$Si).

Elemental analysis data for $C_{30}H_{54}N_4Cl_2Si_4Zr$ (745.25): calculated: C, 48.35; H, 7.30; N, 7.52; Cl, 9.51. Found: C, 48.12; H, 7.59; N, 7.45; Cl, 9.70.

Table 2 Crystal data and refinement details for complexes **12** and **13**

Complex	**12**	**13**
Empirical formula	$C_{28}H_{50}Cl_2N_4O_2Si_4Zr$	$C_{28}H_{50}Cl_2N_4O_2Si_4Zr$
Formula weight	749.20	749.20
Temperature (K)	230.0(1)	230.0(1)
Wavelength (Å)	0.71073	0.71073
Crystal system	Monoclinic	Monoclinic
Space group	*P*21/*c*	*P*21/*c*
Unit cell dimensions	a = 19.409(2) Å b = 11.8110(14) Å c = 17.5870(17) Å α = 90° β = 93.611(8)° γ = 90°	a = 11.7290(4) Å b = 17.8860(6) Å c = 18.8940(7) Å α = 90° β = 92.6470(13)° γ = 90°
Volume (Å^3)	4023.6(7)	3959.4(2)
z, calculated density (Mg m^{-3})	4, 1.237	4, 1.257
Absorption coefficient (mm^{-1})	0.553	0.562
F(000)	1568	1568
Crystal size (mm)	0.39 × 0.39 × 0.30	0.27 × 0.24 × 0.18
θ range for data collection	1.05–23.00	1.57–23.00
Limiting indices	$-21 \le h \le 21$, $-12 \le k \le 12$, $-19 \le l \le 19$	$0 \le h \le 12$, $0 \le k \le 19$, $-0 \le l \le 20$
Reflections collected/unique	9421/5465 [R(int) = 0.0672]	5500/5500 [R(int) = 0.0000]
Completeness to highest θ	97.7%	99.8%
Refinement method	Full-matrix least-squares on F^2	Full-matrix least-squares on F^2
Data/restraints/parameters	5465/0/355	5500/0/370
Goodness-of-fit on F^2	0.902	1.043
Final R indices [$I > 2\sigma(I)$]	R_1 = 0.0600, wR_2 = 0.1523	R_1 = 0.0392, wR_2 = 0.0819
R indices (all data)	R_1 = 0.1171, wR_2 = 0.1757	R_1 = 0.0620, wR_2 = 0.0887
Largest diff. peak and hole (e Å^{-3})	0.745 and −0.522	0.312 and −0.275

[4-^{n}BuC$_6$H$_4$C(NSiMe$_3$)$_2$]$_2$ZrCl$_2$ (11)

1.771 g (4 mmol) of compound **4** gave 1.122 g (70% yield) of **11**.

^{1}H NMR (300 MHz, toluene-d_8): δ = 7.07 (d, ^3J = 8.1 Hz, 4H, Ph), 6.80 (d, ^3J = 8.1 Hz, 4H, Ph), 2.28 (t, ^3J = 7.5 Hz, 4H, CH_2-Ph), 1.32 (quintet, ^3J = 7.5 Hz, 4H, CH_2), 1.12 (sextet, ^3J = 7.3 Hz, 4H, CH_2), 0.78 (t, ^3J = 7.3 Hz, 6H, CH_3), 0.13 (s, 36H, CH_3Si).

^{13}C NMR (75.5 MHz, toluene-d_8): δ = 185.4 (N-*C*-N), 144.6, 137.3, 128.4, 126.2 (Ph), 35.6 (*C*H$_2$-Ph), 33.7 (*C*H$_2$), 22.5 (*C*H$_2$), 14.0 (*C*H$_3$), 2.0 (*C*H$_3$Si).

Elemental analysis data for $C_{34}H_{62}N_4Cl_2Si_4Zr$ (801.6): calculated: C, 50.96; H, 7.80; N, 6.99; Cl, 8.85. Found: C, 48.27; H, 7.99; N, 6.68; Cl, 8.91.

[2-OMeC$_6$H$_4$C(NSiMe$_3$)$_2$]$_2$ZrCl$_2$ (12)

1.667 g (4 mmol) of compound **5** gave 1.229 g (82% yield) of **12**.

^{1}H NMR (300 MHz, toluene-d_8): δ = 7.14 (d, ^3J = 7.5 Hz, 2H, Ph), 6.99 (t, ^3J = 7.5 Hz, 2H, Ph), 6.64 (t, ^3J = 8.3 Hz, 2H, Ph), 6.33 (d, ^3J = 8.3 Hz, 2H, Ph), 3.32 (s, 6H, CH_3-O), 0.22 (s, 18H, CH_3Si), 0.18 (s, 18H, CH_3Si).

^{13}C NMR (75.5 MHz, toluene-d_8): δ = 183.6 (N-*C*-N), 156.5, 131.7, 130.2, 128.6, 121.2, 111.5 (Ph), 55.1 (*C*H$_3$-O), 2.8, 2.3 (*C*H$_3$Si).

Elemental analysis data for $C_{28}H_{50}N_4Cl_2O_2Si_4Zr$ (749.20): calculated: C, 44.89; H, 6.73; N, 7.48; Cl; 9.46. Found: C, 43.91; H, 7.04; N, 7.22; Cl, 9.33.

[3-OMeC$_6$H$_4$C(NSiMe$_3$)$_2$]$_2$ZrCl$_2$ (13)

1.667 g (4 mmol) of compound **6** gave 1.184 g (79% yield) of **13**.

^{1}H NMR (300 MHz, toluene-d_8): δ = 6.93 (m, 2H, Ph), 6.91 (m, 4H, Ph), 6.80 (d, ^3J = 7.6 Hz, 2H, Ph), 6.65 (d, ^3J = 7.6 Hz, 2H, Ph), 3.28 (s, 6H, CH_3-O), 0.20 (s, 36H, CH_3Si).

^{13}C NMR (75.5 MHz, toluene-d_8): δ = 181.4 (N-*C*-N), 159.9, 140.8, 129.8, 118.5, 115.1, 112.0 (Ph), 54.7 (*C*H$_3$-O), 1.9 (*C*H$_3$Si).

Elemental analysis data for $C_{28}H_{50}N_4Cl_2O_2Si_4Zr$ (749.20): calculated: C, 44.89; H, 6.73; N, 7.48; Cl; 9.46. Found: C, 44.57; H, 6.66; N, 7.30; Cl, 9.14.

[(3-C$_4$H$_3$O)C(NSiMe$_3$)$_2$]$_2$ZrCl$_2$ (14)

0.151 g (0.4 mmol) of compound **7** was reacted with 47 mg (0.2 mmol) of $ZrCl_4$ in 5 mL of toluene to give 91 mg (68% yield) of **14**.

^{1}H NMR (500 MHz, toluene-d_8): δ = 6.98 (m, 2H, 5-furyl C-*H*), 6.79 (t, J = 1.6 Hz, 2H, 2-furyl C-*H*), 6.04 (dd, J = 1.6 Hz, J = 0.8 Hz, 2H, 4-furyl C-*H*), 0.19 (s, 36H, CH_3Si).

^{13}C NMR (126.7 MHz, toluene-d_8): δ = 169.4 (N-*C*-N), 152.9 (5-furyl), 142.6 (2-furyl), 139.9 (3-furyl), 110.2 (4-furyl), 1.9 (*C*H$_3$Si).

Elemental analysis data for $C_{22}H_{42}N_4Cl_2O_2Si_4Zr$ (669.08): calculated: C, 39.49; H, 6.33; N, 8.37; Cl, 10.60. Found: C, 38.93; H, 6.66; N, 8.18; Cl, 11.16.

General procedure for the polymerization of propylene[12]

10 mg of the corresponding complex, 1 : 1000 (metal : Al ratio) of MAO and 6 mL of toluene were mixed and loaded into a stainless steel reactor in a glove box. The reactor was connected to the high vacuum line, and 30 mL of propylene was condensed into the reactor. The reactor was warmed to room temperature and stirred vigorously for 3 h. After this period of time the reactor was opened in a well-ventilated hood to exhaust any excess of propylene gas, followed by the addition of a HCl : methanol (15 : 85) mixture to quench the reaction. The resulting polymer was washed with methanol followed by water, aqueous 10% NaOH solution, water and acetone. The polymer was dried in a vacuum oven at 65 °C and the resulting polymer was fractionalized from hexane/ether using a Soxhlet apparatus.[28]

Results and discussion

Synthesis of ligands

The ligands [4-OMeC$_6$H$_4$C(NSiMe$_3$)$_2$]Li·TMEDA (**2**), [4-EtC$_6$H$_4$C-(NSiMe$_3$)$_2$]Li·TMEDA (**3**) and [4-^{n}BuC$_6$H$_4$C(NSiMe$_3$)$_2$]Li·TMEDA

(**4**), [2-OMeC$_6$H$_4$C(NSiMe$_3$)$_2$]Li·TMEDA (**5**), [3-OMeC$_6$H$_4$C-(NSiMe$_3$)$_2$]Li·TMEDA (**6**)[24] and [(3-C$_4$H$_3$O)C(NSiMe$_3$)$_2$] Li·TMEDA (**7**)[25] were prepared by the addition of the corresponding nitriles to an equimolar hexane solution of lithium bis(trimethylsilyl) amide, followed by the addition of an excess of TMEDA to obtain the crystalline ligands **2–7** as described in the literature (eqn (1)).

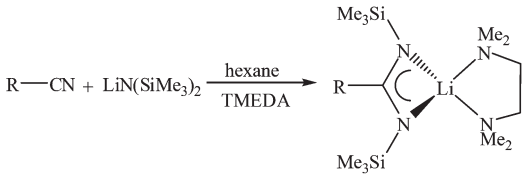

(1)

2 R = 4-OMePh
3 R = 4-EtPh
4 R = 4-^{n}BuPh
5 R = 2-OMePh
6 R = 3-OMePh
7 R = 3-Furyl

Synthesis and structure of complexes

The zirconium bis(benzamidinate)dichloride complexes (**8–14**) were prepared by reacting $ZrCl_4$ with the corresponding lithium amidinates in toluene (eqn (2)).

1-7

(2)

8 R = Ph
9 R = 4-OMePh
10 R = 4-EtPh
11 R = 4-^{n}BuPh
12 R = 2-OMePh
13 R = 3-OMePh
14 R = 3-Furyl

The bis(arylamidinate)zirconium dichloride complexes (**9** (Fig. 1), **11** (Fig. 3), **12** (Fig. 4) and **13** (Fig. 5)) in the solid state, exhibit a slightly distorted *cis* C_2 octahedral geometry, whereas complex **10** (Fig. 2) is fully symmetric with the expected C_2 symmetry. All the complexes are structurally similar to the corresponding titanium complexes reported earlier.[14] The two arylamidinate ligands create two nearly orthogonal N–C–N–Zr rings with the two chlorides situated at a *cis* configuration.

All the M–N bonds (complex **9**: Zr(1)–N(1) = 2.224(2); Zr(1)–N(2) = 2.206(2); Zr(1)–N(3) = 2.251(2); Zr(1)–N(4) = 2.202(2), complex **10**: Zr(1)–N(1) = 2.202(2); Zr(1)–N(2) = 2.233(2), complex **11**: Zr(1a)–N(1a) = 2.206(4); Zr(1a)–N(2a) = 2.213(4); Zr(1a)–N(3a) = 2.221(4); Zr(1a)–N(4a) = 2.225(4), complex **12**: Zr(1)–N(1) = 2.232(6); Zr(1)–N(2) = 2.182(5); Zr(1)–N(3) = 2.206(5); Zr(1)–N(4) = 2.209(6) and complex **13**: Zr(1)–N(1) = 2.239(3); Zr(1)–N(2) = 2.200(3); Zr(1)–N(3) = 2.208(3); Zr(1)–N(4) = 2.234(3)) are very similar and are comparable to those found in previously reported amidinate zirconium complexes.[11c–e,15] In addition, the aromatic ring at the central amidinate carbon

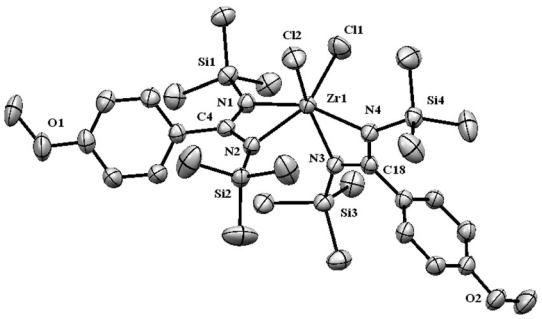

Fig. 1 ORTEP picture of the molecular structure of complex **9** (50% probability ellipsoids). Hydrogen atoms are omitted for clarity. Representative bond lengths (Å) and angles (°): Zr(1)–N(1) = 2.224(2); Zr(1)–N(2) = 2.206(2); Zr(1)–N(3) = 2.251(2); Zr(1)–N(4) = 2.202(2); Zr(1)–Cl(2) = 2.4234(8); Zr(1)–Cl(1) = 2.4219(8); C(4)–N(1) = 1.342(3); C(4)–N(2) = 1.337(3); Si(1)–N(1) = 1.765(2) Å; N(1)–Zr(1)–N(2) = 61.30(8); N(1)–Zr(1)–N(3) = 94.82(8); N(4)–Zr(1)–Cl(1) = 96.78(6); Cl(1)–Zr(1)–Cl(2) = 95.17(3); N(2)–C(4)–N(1) = 115.1(2); N(1)–Zr(1)–N(2)–C(4) = 7.13; N(3)–Zr(1)–N(4)–C(18) = 0.27°.

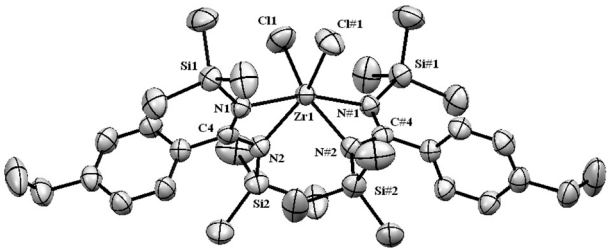

Fig. 2 ORTEP picture of the molecular structure of complex **10** (50% probability ellipsoids). Hydrogen atoms are omitted for clarity. Representative bond lengths (Å) and angles (°): Zr(1)–N(1) = 2.202(2); Zr(1)–N(2) = 2.233(2); Zr(1)–Cl(1) = 2.4089(9); C(4)–N(1) = 1.326(4); C(4)–N(2) = 1.339(3); Si(1)–N(1) = 1.762(2) Å; N(1)–Zr(1)–N(2) = 61.27(8); N(1)–Zr(1)–Cl(1) = 92.74(6); Cl(1)–Zr(1)–Cl#(1) = 97.38(5); N(1)–C(4)–N(2) = 116.0(2); N(1)–Zr(1)–N(2)–C(4) = 7.03°.

in all the complexes is positioned almost perpendicular to the plane of the amidine (N–C═N) motif, eliminating possible resonance effects with the metal center. The crystal data and refinement details for complexes **9–13** are summarized and given in Tables 1 and 2.

Due to the C_2 symmetry, two kinds of nitrogen atoms can be distinguished in the bis amidinate complexes, noted a and b (Fig. 6). As can be seen in Fig. 1–5, the amidinate C–N bond lengths (*ca.* 1.30 Å) are nearly uninfluenced by the type of amidinate carbon substituent. The bond lengths of the central metal to the chlorine atoms are also unchanged considerably as a function of the carbon substitution in all the complexes.

Similar to the two nitrogen types, two different TMS groups also exist: a TMS$_{syn}$ close to the chloride moieties and the corresponding TMS$_{anti}$. In solution, all complexes (except complex **12**), have only one signal for the TMS protons (or carbons) nuclei, contrarily to the different chemical shifts which can be anticipated based on the solid state structures, suggesting that a dynamic racemization ($\Delta \leftrightarrow \Lambda$) process is operative at room temperature for these complexes.[29]

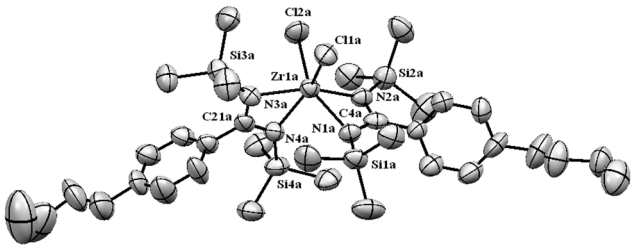

Fig. 3 ORTEP picture of the molecular structure of complex **11** (50% probability ellipsoids). Hydrogen atoms are omitted for clarity. Representative bond lengths (Å) and angles (°): Zr(1a)–N(1a) = 2.206(4); Zr(1a)–N(2a) = 2.213(4); Zr(1a)–N(3a) = 2.221(4); Zr(1a)–N(4a) = 2.225(4); Zr(1a)–Cl(2a) = 2.4151(16); Zr(1a)–Cl(1a) = 2.4221(15); C(4a)–N(1a) = 1.340(6); C(4a)–N(2a) = 1.337(6); Si(1a)–N(1a) = 1.755(4) Å; N(1a)–Zr(1a)–N(2a) = 61.45(15); N(3a)–Zr(1a)–N(1a) = 115.52(17); N(4a)–Zr(1a)–Cl(2a) = 101.57(12); Cl(1a)–Zr(1a)–Cl(2a) = 96.33(6); N(2a)–C(4a)–N(1a) = 115.0(5); N(3a)–Zr(1a)–N(4a)–C(21a) = 0.01; N(1a)–Zr(1a)–N(2a)–C(4a) = 10.09°.

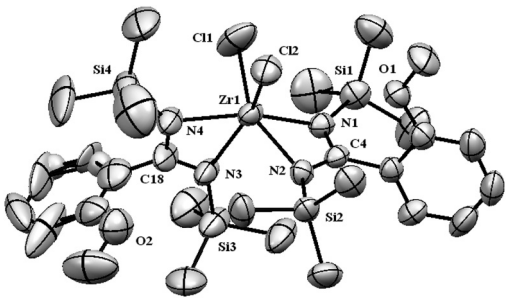

Fig. 4 ORTEP picture of the molecular structure of complex **12** (50% probability ellipsoids). Hydrogen atoms are omitted for clarity. Representative bond lengths (Å) and angles (°): Zr(1)–N(1) = 2.232(6); Zr(1)–N(2) = 2.182(5); Zr(1)–N(3) = 2.206(5); Zr(1)–N(4) = 2.209(6); Zr(1)–Cl(2) = 2.427(2); Zr(1)–Cl(1) = 2.420(2); C(4)–N(1) = 1.344(8); C(4)–N(2) = 1.330(8); Si(1)–N(1) = 1.740(6) Å; N(3)–Zr(1)–N(4) = 61.4(2); N(3)–Zr(1)–N(1) = 96.4(2); N(4)–Zr(1)–Cl(2) = 91.75(16); Cl(1)–Zr(1)–Cl(2) = 95.93(9); N(2)–C(4)–N(1) = 116.6(6); N(3)–Zr(1)–N(4)–C(18) = 2.41; N(1)–Zr(1)–N(2)–C(1) = 9.13°.

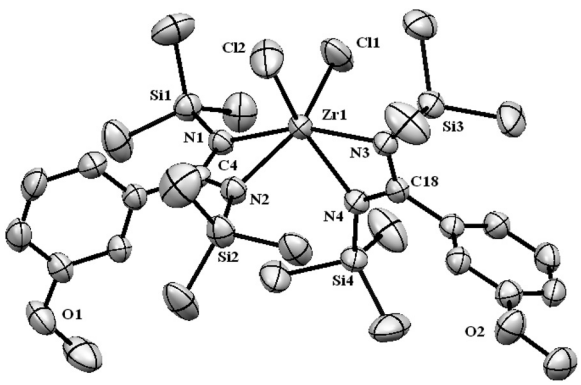

Fig. 5 ORTEP picture of the molecular structure of complex **13** (50% probability ellipsoids). Hydrogen atoms are omitted for clarity. Representative bond lengths (Å) and angles (°): Zr(1)–N(1) = 2.239(3); Zr(1)–N(2) = 2.200(3); Zr(1)–N(3) = 2.208(3); Zr(1)–N(4) = 2.234(3); Zr(1)–Cl(2) = 2.4164(12); Zr(1)–Cl(1) = 2.4202(12); C(4)–N(1) = 1.336(4); C(4)–N(2) = 1.326(4); Si(1)–N(1) = 1.763(3) Å; N(3)–Zr(1)–N(4) = 89.23(11); N(3)–Zr(1)–N(1) = 159.69(10); N(4)–Zr(1)–Cl(2) = 152.08(8); Cl(1)–Zr(1)–Cl(2) = 98.19(5); N(2)–C(4)–N(1) = 116.2(3); N(3)–Zr(1)–N(4)–C(18) = 0.96; N(1)–Zr(1)–N(2)–C(4) = 6.33°.

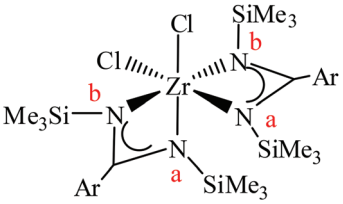

Fig. 6 General structure for complexes **9–13**.

Interestingly, in complex **12**, which is 2-OMe substituted, we observe two signals for the two TMS groups. The lack of similar discrimination among the TMS groups of the 4-OMe and 3-OMe substituted complexes (complexes **9** and **13**, respectively) implies that this effect is not caused by electronic (field, inductive or resonance) substituent effects. Furthermore, the presence of only one set of aryl or substituent-related signals implies that a free rotation of the aromatic ring with respect to the amidinate plane is operative. Three mechanisms can be suggested for the racemization process: a $\kappa^1 \leftrightarrow \kappa^2$ open–close mechanism, a Bailar and a Ray–Dutt twist. The two latter processes involve twisting of the M–N bonds, with no significant involvement of the distal substituted aromatic ring. However, in the $\kappa^1 \leftrightarrow \kappa^2$ process, on the other hand, the chelating ligands open, rearrange, and then close again. It is thus plausible that during the closure process, a TMS group is forced to a closer proximity to the aromatic ring, a step with an expected larger barrier for the *o*-substituted systems. Interestingly, for the titanium complexes with the same ligand or with an *o*-Et or 3-furyl substituent, two signals for the TMS groups were also observed.[15]

Polymerization of propylene

When activated by MAO (polymerization conditions: T = 25 °C, 35 mL C_3H_6(l), 15.5 μmol cat., 1 : 1000 M : Al), all of the examined zirconium amidinate complexes were moderately active in the polymerization of propylene, producing two polymeric fractions: a slightly to low isotactic, ether (or hexane) soluble fraction, which is obtained as a pasty glue, and an ether (or hexane) insoluble fraction, obtained as a moderately to highly isotactic thermoplastic solid. Since each of the fractions is created by a different active species (as presented in the introduction), the polymerization data in Tables 3 and 5 are organized according to the relevant fraction for each complex. For the seven examined zirconium complexes, two fractions were separated by ethereal extraction (extraction with hexane also gave same results). However, the mass percentage of the obtained soluble fraction is lower (*ca.* 49–76%), due to the fact that, as a general rule for benzamidinates, the zirconium complexes showed a larger or comparable activity toward the formation of the solid fraction, and smaller activity toward the formation of the soluble fraction than their titanium counterparts.[14]

Table 3 Data for catalytic polymerization of propylene catalyzed by complexes **8–14** activated by MAO (1 : 1000 M : Al): hexane–ether soluble fraction

Entry	Complex	A^a (10^{-4})	M_w [b]	M_n [c]	PD[d]	R_i [e]	R_t [f]	Ip[g]
1	**8**	0.19	47 600	7000	6.80	0.72	4.3	19.5
2	**9**	0.47	15 050	5000	3.01	1.72	14.5	7.9
3	**10**	0.14	16 080	6000	2.68	0.54	3.8	15.7
4	**11**	0.12	82 440	9000	9.16	0.44	2.0	15.9
5	**12**	0.36	3 793 240	1 628 000	2.33	1.35	0.035	15.9
6	**13**	1.37	15 420	6000	2.57	5.08	35.6	12.6
7	**14**	0.93	51 200	10 000	5.12	3.47	14.6	21.6

[a] Activity ((g of polymer per mole of catalyst)/time). [b] Average molecular weight from GPC analysis (g mol^{-1}). [c] Number-average molecular weight (g mol^{-1}). [d] Polydispersity from GPC analysis. [e] Rate of monomer insertion (mmol h^{-1}). [f] Rate of termination (μmol h^{-1}). [g] Isotactic *mmmm* pentad measured by ^{13}C NMR (%).

Hexane soluble polypropylene fraction

The results of the polymerization experiments for the ether soluble fractions obtained by the zirconium bis(arylamidinates) are shown in Table 3.

The soluble fractions obtained by the zirconium complexes appear as a sticky, wax-like material. Examination of the polymerization results shows a lower activity and, except for complex **9**, higher tacticity as compared to their titanium analogues.[14]

Interestingly, all of the complexes with the oxygen-containing ligands showed higher activities than the complexes with the phenyl or alkyl benzene rings. As can be judged by the very similar molecular weights obtained for the soluble fraction (with the noteworthy exception of complex **12**, entry 5 in Table 3), an increase in the insertion rates is accompanied by a similar increase in the termination rate. The ultrahigh molecular weight obtained by the 2-anisolyl amidinate corresponds to a remarkable *ca.* 3 orders of magnitude decrease in the termination rate when compared to its analogous titanium complex and more than 2 orders of magnitude when compared to the isomeric *p*-OMe substituted analogous zirconium complex, which has similar-through bond-electronic properties.[14]

The isotacticity of the soluble fraction obtained from all of the examined complexes is typically in the range of 7.9–21.6% *mmmm*, which is not significantly larger than the isotacticity of 6.25% expected of a Bernoullian pentad distribution.[30] This low tacticity of the soluble fraction strongly suggests that in all the amidinates, the ligands in the active cationic species have lost most of their stereo-orienting abilities for incoming monomers, most probably due to the transfer of one amidinate ligand from the bisamidinate dimethyl complex to an aluminum center in MAO, with the concurrent formation of a C_1 symmetric monoamidinate complex.[12] In addition, the low termination rate, exhibited by the 2-anisolyl amidinate complex **12**, compared to the other phenyl derivatives, seems to originate from the effect of the pendant heteroatom. The availability of the close pendant heteroatoms can allow the rearrangement of the κ^1 monoamidinate by closing a new chelate, consisting of amidinate nitrogen and the heteroatom (Fig. 7). The low termination rate of these new active species as compared to the phenyl derivatives may stem from both steric and electronic reasons.

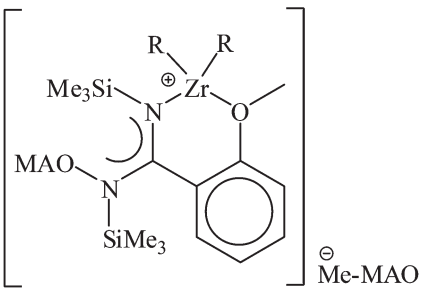

Fig. 7 Formation of κ^1 amidinate complex in the case of **12**.

Unlike the analogues titanium complexes,[14] an attempt to find any LFER (linear free energy relationships) for the normalized insertion or termination rates for both the fractions obtained by the zirconium catalysts did not bear fruit, suggesting that the combination of steric and electronic substituent effects is indeed operative. Further, particularly for complexes **8**, **11** and **14**, a multi-site catalytic system is obtained, as suggested by the high polydispersity indices of the obtained polymers.[31]

Analysis of the misinsertion rates for the ether soluble fraction obtained by zirconium arylamidinates

Among the important factors that influence the mechanical properties of the polymer, beside the tacticity and molecular weights, is the frequency of the Et and ^{n}Bu segments in the chain, which results from 2,1- and 3,1-insertion processes.[32,33] These linear segments can form crystalline areas in the polymer bulk, similar to those in ethylene–propylene rubber, which serve as non-covalent cross-linkages between chains, resulting in the formation of an elastomeric polymer even if its molecular weight and tacticity are relatively low. The detection of these chain microstructures is achieved through analysis of the ^{13}C NMR spectrum of the polymer, in which the Et and ^{n}Bu segments appear as wide signals in the ranges of 30.6–31.5 ppm and 35.1–36.2 ppm, respectively.[34,35] The

Table 4 2,1- and 3,1-insertion rates for the ether–hexane soluble fraction

Entry	Complex	$r_{2,1}$ [a] × 10 (mmol min^{-1})	$r_{3,1}$ [b] × 10 (mmol min^{-1})	$X_{2,1}$ [c] (%)
1	**8**	0.33	0.079	2.7
2	**9**	1.07	0.31	3.7
3	**10**	0.43	0.14	4.8
4	**11**	0.23	0.066	3.2
5	**12**	1.06	0.32	4.7
6	**13**	1.64	0.42	1.9
7	**14**	2.57	0.78	4.4

[a] The 2,1 insertion rate. [b] The 3,1 insertion rate. [c] The frequency of the 2,1 insertion among all insertions (determined by NMR).

two vicinal methyl groups which are also obtained as a result of 1,2-2,1-1,2 (or 2,1-1,2-2,1) insertion events resonate at the ppm ranges of 14.5–15.7 and 16.6–17.7, which correspond to the *r* and *m* diads for these methyl groups, respectively.[34,35]

In all of the examined soluble fractions, obtained from all the seven zirconium complexes, 2,1- and 3,1-insertions were responsible for the majority of the special chain segments (*i.e.*, not part of the regular [CH_2–$CHCH_3$] chain). As can be seen in Table 4, the frequencies of the 2,1 insertion, $X_{2,1}$ (eqn (3)), are similar for all the complexes, regardless of the ligand, with an average of 3.7% (σ = 1.1) (σ – the standard deviation). This lower rate of 2,1 insertion in these zirconium complexes partially explains the appearance of the soluble fractions catalyzed by them as sticky and waxy pastes.

Inspection of the rates for the 2,1- and 3,1-insertions (calculated using eqn (3) and (4), respectively, and listed in Table 4) reveals a surprising linear correlation between these rates for the complexes, regardless of the ligand (Fig. 8).

$$r_{2,1} = \mathrm{ri} \times \mathrm{X}_{2,1} = \mathrm{ri} \times \frac{0.5 \times I_{\mathrm{Et}}}{0.5 \times I_{\mathrm{Bu}} + I_{\mathrm{Et}} + I_{\mathrm{CH_2}}} = \frac{m_{\mathrm{pp}}}{t \times M_{\mathrm{w}}(\mathrm{p})} \times \frac{0.5 \times I_{\mathrm{Et}}}{0.5 \times I_{\mathrm{Bu}} + I_{\mathrm{Et}} + I_{\mathrm{CH_2}}} \quad (3)$$

$$r_{3,1} = \mathrm{ri} \times \mathrm{X}_{3,1} = \mathrm{ri} \times \frac{0.25 \times I_{Bu}}{0.5 \times I_{\mathrm{Bu}} + I_{\mathrm{Et}} + I_{\mathrm{CH_2}}} = \frac{m_{\mathrm{pp}}}{t \times M_{\mathrm{w}}(\mathrm{p})} \times \frac{0.25 \times I_{\mathrm{Bu}}}{0.5 \times I_{\mathrm{Bu}} + I_{\mathrm{Et}} + I_{\mathrm{CH_2}}} \quad (4)$$

where ri is the total insertion rate, *X* is the mol fraction, m_{pp} is the fraction mass, *I* is the integral value (normalized to I_{mmmm} = 1); Et, Bu and CH_2 represent the relevant region in the spectrum, *t* is the polymerization time, M_{w}(p) is the M_{w} of the monomer (propylene).

A simple extraction of the rate for the 3,1 insertion from the linear regressions shows that only *ca.* 30% of the 2,1 insertions continue to the 3,1 path to produce the ^{n}Bu segment. This lower percentage of the ^{n}Bu segment indicates the more amorphous nature of these polymers.

The linear dependence of the 3,1 insertion rate on the 2,1 rate suggests that the $r_{2,1\text{-}1,2}$ (rate for a 2,1 insertion after 1,2 insertion) (Scheme 2), $r_{1,2\text{-}2,1}$ (1,2 after 2,1), $r_{3,1}$ (and other rates of plausible processes, such as $r_{2,1\text{-}2,1}$, if operative) are influenced for the central metal in a similar manner by external factors such as ligands or solvents (which act by adding themselves as ligands or by removing other ligands such as propylene or MAO methyl or oxygen moieties). The low occurrence of the 3,1 insertions in these zirconium complexes is thus probably a result of the interaction of the incoming monomer and/or growing chain with the 4d orbital of the zirconium.

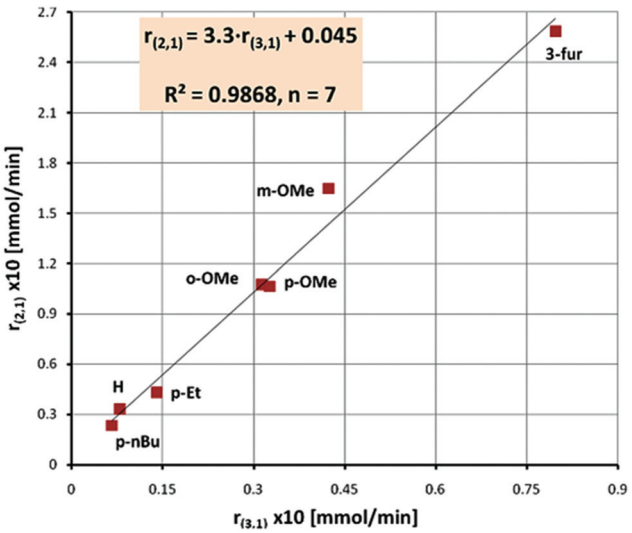

Fig. 8 Linear correlation between the 2,1 and 3,1 rates [mmol min^{-1}] for the elastomeric fraction produced by the Zr complexes (**8–14**).

Hexane insoluble polypropylene fraction

The results of the polymerization experiments for the ether insoluble fraction obtained by the zirconium bis(arylamidinates) are shown in Table 5. Inspection of the yields of the insoluble fraction reveals that similar to the situation for the soluble fraction, the zirconium complexes with the oxygen-containing ligands showed higher activities than the complexes with the phenyl or alkyl benzene rings. Pentad analysis reveals that the solid fraction is a blend of a predominantly isotactic (*ca.* 61–71% *mmmm*) polymer, with the characteristic ideal block microstructure obtained by site-control, and a moderately syndiotactic (*ca.* 36–49% *rrrr*) polymer, with a chain-end control of the stereochemistry, as suggested by the 1 : 1 integration ratio between the *rrrm* and *rmrr* pentads[36,37] (Fig. 9). This latter syndiotactic fraction forms *ca.* 13–38% of the polymer mass, as determined by NMR. These two types of polymers are clearly produced by at least two types of active sites, as also reflected by the high value of the polydispersity indices.[31] This syndiotactic fraction is produced by an amidinate-containing species (not yet identified), as suggested by the variation of its yield as a function of substitution.

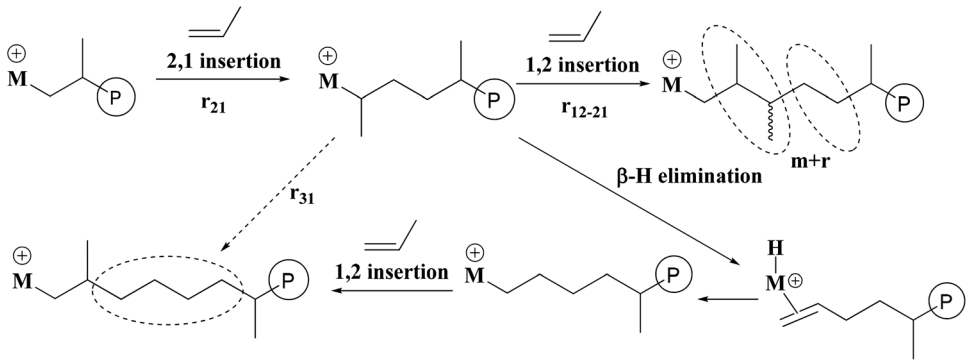

Scheme 2 General mechanism for the formation of the 2,1 and 3,1 segments in the polypropylene chain.

Table 5 Data for catalytic polymerization of propylene catalyzed by complexes **8–14** activated by MAO (1 : 1000 M : Al): hexane–ether insoluble fraction

Entry	Complex	A^a (10^{-4})	M_w [b]	M_n [d]	PD[c]	R_i [e]	R_t [f]	Ip[g] (%)	Iso yield[h] (%)	SP[i] (%)	Syndio yield[j] (%)
1	**8**	0.15	75 000	12 000	6.25	0.56	2.0	63.5	62.1	48.4	37.9
2	**9**	0.43	55 200	23 000	2.4	1.58	2.95	61.4	67.2	53.8	32.8
3	**10**	0.12	108 080	14 000	7.72	0.44	1.35	62.0	80.1	35.9	19.9
4	**11**	0.12	125 100	9000	13.9	0.44	2.1	67.2	72.9	49.2	27.1
5	**12**	0.21	117 280	8000	14.66	0.75	4.1	71.0	82.7	48.7	17.3
6	**13**	0.43	17 220	7000	2.46	1.57	9.7	66.1	86.8	40.0	13.2
7	**14**	0.35	90 860	11 000	8.24	1.11	4.8	65.0	84.2	42.8	15.8

[a] Activity ((g of polymer per mole of catalyst)/time). [b] Average molecular weight from GPC analysis (g mol^{-1}). [c] Number-average molecular weight (g mol^{-1}). [d] Polydispersity from GPC analysis. [e] Rate of monomer insertion (mmol h^{-1}). [f] Rate of termination (μmol h^{-1}). [g] % *mmmm*. [h] Isotactic fraction yield (by NMR). [i] % *rrrr*. [j] Syndiotactic fraction yield (by NMR).

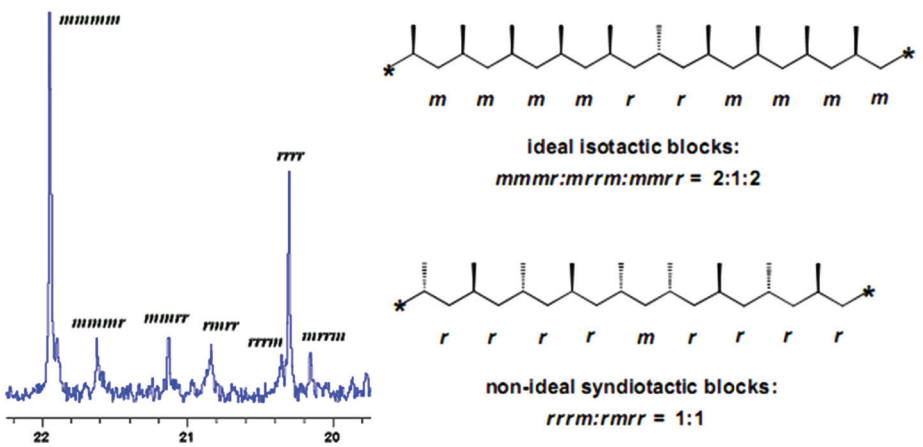

Fig. 9 ^{13}C NMR spectrum of the methyl region of the solid fraction obtained from complex **10**, showing the assignment of pentads for the two kinds of polypropylenes.

Conclusions

Various bis(*N*,*N*-trimethylsilylarylamidinate)zirconium dichloride complexes with different aryl substituents were prepared. The *ortho* aromatic substituent raises the activation barrier for the site racemization process (Δ ↔ Λ), as reflected in the existence of the examined *o*-substituted complex as a racemic mixture at room temperature, whereas in the other complexes, the racemization rate at room temperature is fast on the NMR time scale.

The high-pressure propylene (liquid propylene) polymerization promoted by these substituted zirconium aryl amidinates after their activation by MAO provided two fractions after ethereal extraction. All of the ether soluble polymers obtained by the zirconium complexes were sticky polymers with lower molecular weight and at lower activity. However, we were not successful in rationalizing the noticeable substituent effect (linear free energy relationship (LFER) between various electronic substituent parameters and log [Ri(*x*)] or log [Rt(*x*)]).

The solid fraction of the polymers formed by the zirconium catalyst (*ca*. 50% of the whole polymer) was composed of two polymer types: (identified by pentad analysis *via* ^{13}C NMR) a highly isotactic polymer, formed by a site-control mechanism, and a moderately syndiotactic polymer (*rrrr* ≈ 40–50%) formed by a chain-end control. When a close pendant heteroatom is present (an *o*-substituted phenyl), rearrangement of the amidinate ligand in the mono amidinate cationic species to a κ^1 mode and coordination of the heteroatom forms new chelates which induces a polymer with a very high molecular weight as compared to those observed for the phenyl derivatives. Interestingly, a linear correlation was found between the rates of the 2,1 and 3,1 insertions for the soluble fractions obtained. This correlation was not affected by the ligand substituents.

Acknowledgements

This research was supported by the USA–Israel Binational Science Foundation under contract 2008283. S.A. thanks Raymond Rosen for a graduate fellowship.

References

1 (*a*) *Metallocene-Based Polyolefins. Preparation, Properties and Technology*, ed. J. Scheirs and W. Kaminsky, Wiley, New York, 1999, vol. 1; (*b*) *Metallocene-Based Polyolefins*, ed. J. Scheirs and W. Kaminsky, Wiley, Chichester, 2000, vol. 2; (*c*) *Topics in Catalysis*, ed. T. J. Marks and J. C. Stevens, Baltzer, Basel, Switzerland, 1999, vol. 15; (*d*) W. Kaminsky, Olefin Polymerization Catalyzed by Metallocenes, in *Advances in Catalysis*, ed. B. C. Gates and H. Knozinger, Academic Press, San Diego, 2002, vol. 46, p. 89.

2 (*a*) G. Fink, B. Steinmetz, J. Zechlin, C. Przybyla and B. Tesche, *Chem. Rev.*, 2000, **100**, 1377; (*b*) Y. Qian, J. Huang, M. D. Bala, B. Lian, H. Zhang and H. Zhang, *Chem. Rev.*, 2003, **103**, 2633; (*c*) E. Y.-X. Chen and T. J. Marks, *Chem. Rev.*, 2000, **100**, 1391; (*d*) M. Delferro and T. J. Marks, *Chem. Rev.*, 2011, **111**, 2450; (*e*) A. Razavi and U. Thewalt, *Coord. Chem. Rev.*, 2006, **250**, 155; (*f*) G. W. Coates, *Chem. Rev.*, 2000, **100**, 1223.

3 (*a*) W. Kaminsky and M. Arndt, *Adv. Polym. Sci.*, 1997, **127**, 143; (*b*) K. Mashima, Y. Nakayama and A. Nakamura, *Adv. Polym. Sci.*, 1997, **133**, 1.

4 (*a*) H. Braunschweig and F. M. Breitling, *Coord. Chem. Rev.*, 2006, **250**, 2691; (*b*) G. J. P. Britovsek, V. C. Gibson and D. F. Wass, *Angew. Chem., Int. Ed.*, 1999, **38**, 428; (*c*) A. L. McKnight and R. M. Waymouth, *Chem. Rev.*, 1998, **98**, 2587.

5 (*a*) L. Wang, Q. Wu, H. Xu and Y. Mu, *Dalton Trans.*, 2012, **41**, 7350; (*b*) M. Erben, J. Merna, O. Hylsky, J. Kredatusova, A. Lycka, L. Dostal, Z. Padelkova and M. Novotny, *J. Organomet. Chem.*, 2013, **725**, 5; (*c*) K. Nomura, J. Liu, S. Padmanabhan and B. Kitiyanan, *J. Mol. Catal. A: Chem.*, 2007, **267**, 1; (*d*) X. Y. Tang, Y. X. Wang, S. R. Liu, J. Y. Liu and Y. S. Li, *Dalton Trans.*, 2013, **42**, 499.

6 (*a*) J. Wei, W. Hwang, W. Zhang and L. R. Sita, *J. Am. Chem. Soc.*, 2013, **135**, 2132; (*b*) L. R. Sita, *Angew. Chem., Int. Ed.*, 2011, **50**, 6963.

7 (*a*) V. C. Gibson and S. K. Spitzmesser, *Chem. Rev.*, 2003, **103**, 283; (*b*) S. Collins, *Coord. Chem. Rev.*, 2011, **255**, 118.

8 (*a*) S.-D. Bai, F. Guan, M. Hu, S.-F. Yuan, J.-P. Guo and D.-S. Liu, *Dalton Trans.*, 2011, **40**, 7686; (*b*) V. Busico, R. Cipullo, L. Caporaso, G. Angelini and A. L. Segre, *J. Mol. Catal. A: Chem.*, 1998, **128**, 53; (*c*) G. Li, M. Lamberti, G. Roviello and C. Pellecchia, *Organometallics*, 2012, **31**, 6772; (*d*) X.-C. Shi and G.-X. Jin, *Organometallics*, 2012, **31**, 7198; (*e*) N. Suzuki, G. Kobayashi, T. Hasegawa and Y. Masuyama, *J. Organomet. Chem.*, 2012, **717**, 23; (*f*) D. Takeuchi, *Dalton Trans.*, 2010, **39**, 311; (*g*) Y. Yoshida, S. Matsui, Y. Takagi, M. Mitani, T. Nakano, H. Tanaka, N. Kashiwa and T. Fujita, *Organometallics*, 2001, **20**, 4793.

9 (*a*) E. Smolensky and M. S. Eisen, *Dalton Trans.*, 2007, 5623; (*b*) C. Averbuj, E. Tish and M. S. Eisen, *J. Am. Chem. Soc.*, 1998, **120**, 8640; (*c*) V. Volkis, M. Shmulinson, E. Shaviv, A. Lisovskii, D. Plat, O. Kuhl, T. Koch, E. Hey-Hawkins and M. S. Eisen, PMSEP reprints, 223rd ACS National Meeting, Orlando, FL, April 7–11, 2002, American Chemical Society, Washington, DC, 2002, **86**, 301; (*d*) M. Sharma, H. S. Yameen, B. Tumanskii, S.-A. Filimon, M. Tamm and M. S. Eisen, *J. Am. Chem. Soc.*, 2012, **134**, 17234.

10 (*a*) D. A. Kissounko, M. V. Zabalov, G. P. Brusova and D. A. Lemenovskii, *Russ. Chem. Rev.*, 2006, **75**, 351; (*b*) F. T. Edelmann, *Adv. Organomet. Chem.*, 2008, **57**, 183.

11 (*a*) E. Nelkenbaum, M. Kapon and M. S. Eisen, *Organometallics*, 2005, **24**, 2645; (*b*) E. Domeshek, R. J. Batrice, S. Aharonovich, B. Tumanskii, M. Botoshansky and M. S. Eisen, *Dalton Trans.*, 2013, **42**, 9069; (*c*) V. Volkis, M. Shmulinson, C. Averbuj, A. Lisovskii, F. T. Edelmann and M. S. Eisen, *Organometallics*, 1998, **17**, 3155; (*d*) D. Herskovics-Korine and M. S. Eisen, *J. Organomet. Chem.*, 1995, **503**, 307; (*e*) V. Volkis, E. Nelkenbaum, A. Lisovskii, G. Hasson, R. Semiat, M. Kapon, M. Botoshansky, Y. Eishen and M. S. Eisen, *J. Am. Chem. Soc.*, 2003, **125**, 2179; (*f*) J. Richter, F. T. Edelmann, M. Noltemeyer, H.-G. Schmidt, M. Shmulinson and M. S. Eisen, *J. Mol. Catal. A: Chem.*, 1998, **130**, 149; (*g*) E. Otten, P. Dijkstra, C. Visser, A. Meetsma and B. Hessen, *Organometallics*, 2005, **24**, 4374.

12 V. Volkis, A. Lisovskii, B. Tumanskii, M. Shuster and M. S. Eisen, *Organometallics*, 2006, **25**, 2656.

13 (*a*) S. Aharonovich, V. Volkis and M. S. Eisen, *Macromol. Symp.*, 2007, **260**, 165; (*b*) V. Volkis, S. Aharonovich and M. S. Eisen, *Macromol. Res.*, 2010, **18**, 967.

14 S. Aharonovich, M. Botoshansky, Y. S. Balazs and M. S. Eisen, *Organometallics*, 2012, **31**, 3435.

15 S Aharonovich, *Heteroaza-allyl Complexes of Li, Ti, Zr, and V: Structure, Reactivity and Catalytic Propylene Polymerization*, Ph.D. Thesis, Technion-Israel Institute of Technology, 2010.

16 (*a*) S. Matsui and T. Fujita, *Catal. Today*, 2001, **66**, 63; (*b*) S. Matsui, Y. Inoue and T. Fujita, *J. Synth. Org. Chem., Jpn.*, 2001, **59**, 232.
17 (*a*) E. Y. Tshuva, S. Groysman, I. Goldberg, M. Kol and Z. Goldschmidt, *Organometallics*, 2002, **21**, 662; (*b*) H. Nakazawa, S. Ikai, K. Imaoka, Y. Kai and T. Yano, *J. Mol. Catal. A: Chem.*, 1998, **132**, 33.
18 (*a*) S. Doherty, R. J. Errington, A. P. Jarvis, S. Collins, W. Clegg and M. R. J. Elsegood, *Organometallics*, 1998, **17**, 3408; (*b*) M. Shmulinson, M. Galan-Fereres, A. Lisovskii, E. Nelkenbaum, R. Semiat and M. S. Eisen, *Organometallics*, 2000, **19**, 1208.
19 *Kappa CCD Server Software*, Nonius BV, Delft, The Netherlands, 1997.
20 Z. Otwinowski and W. Minor, *Methods Enzymol.*, 1997, **276**, 307.
21 G. M. Sheldrick, *Acta Crystallogr., Sect. A: Fundam. Crystallogr.*, 1990, **46**, 467.
22 *ORTEP, TEXSAN Structure Analysis Package*, Molecular Structure Corp., The Woodlands, TX, 1999.
23 http://www.ccdc.cam.ac.uk/Solutions/CSDSystem/Pages/Mercury.aspx
24 S. Aharonovich, M. Kapon, M. Botoshanski and M. S. Eisen, *Organometallics*, 2008, **27**, 1869.
25 S. Aharonovich, M. Botoshanski, Z. Rabinovich, R. M. Waymouth and M. S. Eisen, *Inorg. Chem.*, 2010, **49**, 1220.
26 J. R. Hagadorn and J. Arnold, *J. Chem. Soc., Dalton Trans.*, 1997, 3087.
27 R. Gomez, R. Duchateau, A. N. Chernega, A. Meetsma, F. T. Edelmann, J. H. Teuben and M. L. H. Green, *J. Chem. Soc., Dalton Trans.*, 1995, 217.
28 I. Pasquin, *Pure Appl. Chem.*, 1967, **15**, 465.
29 T. Elkin, S. Aharonovich, M. Botoshansky and M. S. Eisen, *Organometallics*, 2012, **31**, 7404.
30 M. Farina, *Top. Stereochem.*, 1987, **17**, 1.
31 (*a*) A. E. Hamielec and J. B. P. Soares, *Prog. Polym. Sci.*, 1996, **21**, 651; (*b*) D. Liguori, R. Centore, A. Tuzi, F. Grisi, I. Sessa and A. Zimbelli, *Macromolecules*, 2003, **36**, 5451.
32 L. Resconi, L. Cavallo, A. Fait and F. Piemontesi, *Chem. Rev.*, 2000, **100**, 1253.
33 (*a*) J. D. Azoulay, H. Gao, Z. A. Koretz, G. Kehr, G. Erker, F. Shimizu, G. B. Galland and G. C. Bazan, *Macromolecules*, 2012, **45**, 4487; (*b*) E. F. McCord, S. J. McLain, L. T. J. Nelson, S. D. Ittel, D. Tempel, C. M. Killian, L. K. Johnson and M. Brookhart, *Macromolecules*, 2007, **40**, 410.
34 S. E. Ewart, M. J. Sarsfield, D. Jeremic, T. L. Tremblay, E. F. Williams and M. C. Baird, *Organometallics*, 1998, **17**, 1502.
35 V. Busico and R. Cipullo, *Prog. Polym. Sci.*, 2001, **26**, 443.
36 G. H. Llinas, S. H. Dong, D. T. Mallin, M. D. Rausch, Y. G. Lin, H. H. Winter and J. C. W. Chien, *Macromolecules*, 1992, **25**, 1242.
37 J. A. Ewen, *J. Am. Chem. Soc.*, 1984, **106**, 6355.

